Key Engineering Materials
ISSN: 1662-9795, Vol. 926, pp 1650-1659
doi:10.4028/p-04tr68

Submitted: 2021-12-08
Revised: 2022-01-25
Accepted: 2022-02-02
Online: 2022-07-22

Experimental Analysis of Cirrcular Milling for Material Identification in Aerospace Industry

Sughosh Deshpande[a*], Anna Carla Araujo[b], Pierre Lagarrigue[c], and Yann Landon[d]

Institut Clément Ader, Université de Toulouse, CNRS/INSA/ISAE/Mines Albi/UPS, France

[a]sughosh.deshpande@univ-tlse3.fr, [b]araujo@insa-toulouse.fr,
[c]pierre.lagarrigue@univ-jfc.fr, [d]yann.landon@univ-tlse3.fr

Keywords: Smart Machining, Stack Materials, Material Identification, Titanium Alloy, Helical Milling.

Abstract. In the airplane design, thousand holes should be manufactured by machining leading this process in the first place for process optimization. Recently, the stack materials used in this application are sheet layers of Titanium alloy, Aluminum alloy and CFRP, which normally are machined under different cutting conditions. There are two main solutions when drilling stacks: using the more conservative ones or changing the parameters for each layer. In orbital drilling, the forces are lower with better quality but with longer machining time compared to drilling, allowing the measurement and control of the process. Smart machining techniques can be applied for recognising and adapting the cutting parameters in real time, depending on a database for decision-making. In this paper, a technique is proposed to identify the cutting material based on the cutting and feed components of the machining force in a circular milling process. Experiments consist of machining separately Titanium and Aluminium alloy workpieces in a similar range of cutting speed and feed, measuring forces and the position of the cutting tool (X,Y, SP) using the machine-tool data. The results show that it is possible to identify the materials using the calculated tangential and radial force components in the tool referential frame because the values of specific cutting and feed force are significantly different for each material. A specific force map is used as a signature to distinguish the materials in real time machining which can be used for orbital drilling in the next step of the research.

Introduction

Multi stack drilling is one of the major operations in aircraft assemblies and it demands lots of time and resources to achieve high-quality holes. Usually, Titanium and Aluminium stacked materials are drilled before aircraft assembly and this poses a major challenge in machining due to the different machinability of materials. Some of the drilling challenges include poor finishing, burr formation and rapid tool wear [1]. However, hole quality aspects like exit burrs can have a significant influence during assembly and also affect productivity [2].

As an alternative for axial drilling operation, orbital drilling, an helical milling process, can be applied. This process shows advantages regarding the process flexibility and ability to produce high-quality holes on different materials [3, 4]. Sun et al [5] data shows that the fatigue life of holes produced by helical milling showed better life compared to conventional drilling. The burr height at the hole exits was considerably lower in orbital drilling compared to conventional drilling [6]. However, helical milling alone will not completely eliminate the problems faced in stacked hole making operations.

The environmental protection initiatives, such as ISO 14001 and lean manufacturing ideology, push researchers to develop flexible and smart processes to improve efficiency and productivity to reduce costs [7]. It is a fact that thousands of holes have to be drilled for assembling an airplane, so smart drilling is a key point for performance maximization. Hence, increasing the feed rate or cutting speed on the layer that presents higher machinability is directly related to this goal [8].

Smart machining refers to real time adaptation of cutting parameters for process optimization. It involves identifying the material accurately and then adapting the proper cutting parameters in real time for process optimization. In this area, Pardo et al [9] discusses decision making strategies in order

to identify the tool position in stack drilling for adaptation of cutting parameters. A force sensorless method is proposed by Fang et al [10] in stacked orbital drilling of CFRP and Titanium in order to determine the tool position across different layers. Also, Wenkler et al [11] developed a way of predicting specific cutting force by Artificial Neutral Network which can be implemented in process planning or smart manufacturing.

Mechanistic force models can provide quantitative cutting force predictions based on the uncut chip thickness principle. Once experimental tests are made, the cutting force models enable estimating the specific cutting coefficients for a different set of variables. In this area, numerous papers predict cutting forces by considering different factors to improve the model accuracy. Armarego et al [12], for example, developed a force model considering tool run out to accurately predict cutting forces. Montgomery et al [13] included tool workpiece vibrations into the model to calculate cutting forces and specific force coefficients based on the chip load. Geometry of chip formation and prediction of forces in circular milling is discussed by Banerjee et al [14]. Wu et al [15] discussed force models for circular milling taking into account the uncut chip thickness and feed rates variation at the corners. The cutting coefficients calculation in circular milling models can be further extended for helical milling adding vertical feed.

The specific cutting coefficients data can be used to identify the material being machined. They can act as material signatures to adapt proper cutting parameters in real time. These data could directly improve the process productivity and hole quality if appropriate cutting parameters are applied for the specific material. There are many articles proposing methodologies to calculate cutting forces and cutting coefficients, but rarely on a data map of specific force coefficients of different materials. Similar data maps were developed recently by our team for axial drilling [16].

This article proposes a technique for material identification in circular milling process of Aluminium and Titanium alloys used in aerospace industry. Our work also introduces integration of external sensor to identify cutting flute position in real time which can be helpful in smart machining applications.

The materials used for the experiments were Aluminum 2017A and Titanium Ti6Al4V, being subjected to a common set of cutting conditions. In the following sections, the force model and cutting coefficients are presented, along with material and methods, followed by experimental results and identification maps for both the materials.

Force Model and Specific Force Coefficients

The forces for a general orthogonal cutting can be described by a mechanistic force model, as described by [17], considering only cutting action of the cutting edge neglecting ploughing and chisel edge effects.

In this way, the machining force $\vec{F}_m$ is calculated considering the small finite elements of the cutting flute in the cutting edge referential frame decomposed: tangential (dF_c), radial (dF_r) and axial (dF_z) components.

$$d\vec{F}_m = \begin{bmatrix} dF_c \\ dF_r \\ dF_z \end{bmatrix} \tag{1}$$

The local force at point P of the cutting edge is a function of the uncut chip thickness h and the specific force coefficients: K_c, K_r and K_z, as presented in Eq. 1.

$$dF_c = K_c(P).h(P)db \tag{2}$$

$$dF_r = K_r(P).h(P)db \tag{3}$$

$$dF_z = K_z(P).h(P)db \tag{4}$$

where $h(P)db$ is the elementary uncut chip load calculated on the reference point P in db elemental length of the cutting edge.

For each rotating tool machining process, there are some assumptions in order to identify a global value for specific force coefficients: milling and circular milling, as follows in the next subsections.

Milling

In milling, in order to determine the cutting coefficients of the tool-workpiece pair, the local cutting force $dF_c(t)$ and the radial force $dF_r(t)$ are analyzed considering the variation of the uncut chip thickness (h) along the tool rotation.

The angle of local position ϕ of the flute i can be expressed considering the tool helix angle λ, the angle between flutes $\phi_p = \frac{2\pi}{N}$, where N is the number of flutes and a_p the axial depth of cut.

$$\phi(\theta_2, i) = \theta_2 - (i-1)\phi_p \tag{5}$$

Martellotti equation [18] described the chip thickness $h(\phi)$ as a function of feed per tooth (f_z) and ϕ, calculated considering the tool rotation angle (θ_2), and given by the equation:

$$h(\phi) = f_z \sin\left(\phi(\theta_2, i)\right) \tag{6}$$

When summing the force contributions of each elemental cutting part db, $dF_c(t)$ and $dF_r(t)$, the directions are not the same and a change to a fixed referential is necessary. From there, $dF_x(t)$ and $dF_y(t)$ can be calculated.The forces in axial direction (dF_z) can be neglected, if the helix angle is small.

As in any machining process, some assumptions should be made for the identification of specific cutting force and specific radial force. It is considered that the maximum force is achieved in the position of θ_2 when the average uncut chip thickness along the cutting edge is higher. The reference frame is now fixed in the rotating tool θ_2 and not in each element. Then, the approximation done lead to:

$$K_c = \frac{F_c(\theta_2)}{A_c(\theta_2)} \longrightarrow K_c = \frac{F_{c(max)}}{A_{c(max)}} \approx \frac{F_{c(max)}}{h'_{(max)}.a_p} \tag{7}$$

$$K_r = \frac{F_r(\theta_2)}{A_c(\theta_2)} \longrightarrow K_r = \frac{F_{r(max)}}{A_{c(max)}} \approx \frac{F_{r(max)}}{h'_{(max)}.a_p} \tag{8}$$

where A_c is chip cross section area , h'_{max} is maximum uncut chip thickness and a_p is axial depth of cut.

Circular Milling

Unlike in linear milling, circular milling involves movement of tool around a centered fixed point in clockwise or anticlockwise direction to enlarge a existing hole diameter. Figure 1(b) shows the circular milling tool trajectory (at θ_1= 0) and the associated geometric parameters. A tool of diameter D_t with center C is moving around the hole center O. D_1 refers to pre hole diameter and D is the final diameter to be achieved after circular milling. R_{tt} is the tool trajectory radius with reference to hole center O [19].

In circular milling, cutting forces at the cutting edge have different referential frames that have to be analyzed in order to determine the cutting coefficients of the tool-workpiece pair. The cutting forces exerted by the tool on the workpiece can be seen in Figure 1(a). Feed motion produces F_{tan} and F_{rad} forces and the cutting action gives rise to tangential (F_t), radial (F_r) and axial forces (F_z) at the cutting edge. It can be noted that the direction of feed forces in circular milling changes continuously unlike in linear milling where feed direction and feed force direction remain unchanged. In circular milling context, forces in axial direction (F_z) can be neglected.

Figure 2 shows chip formation in circular milling indicating entry and exit of cutting flute with the workpiece. θ_2 is measured from fixed referential frame of rotating tool with flute 1 of the end mill. The angle ψ is the swept angle of the flute which is determined by the entry and exit of the cutting flute as shown in the Fig. 2. The uncut chip thickness varies from h_{min} to h_{max} as the flute rotates

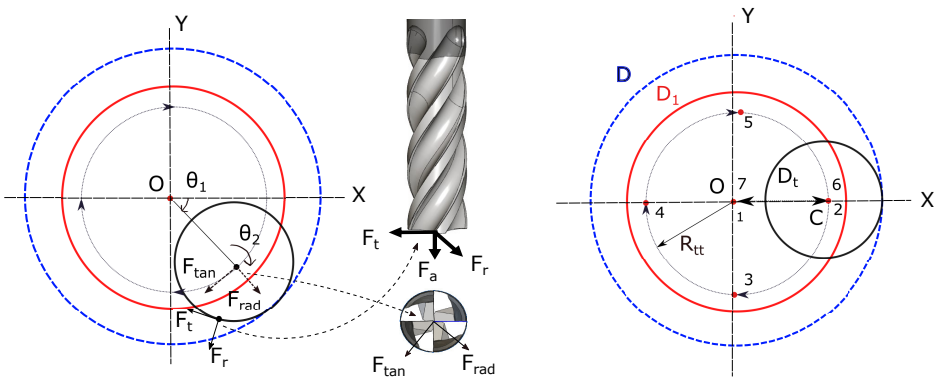

(a) Cutting Forces (b) Tool Trajectory (at θ_1=0)

Fig. 1: Referential Frames in X and Y indicating cutting forces and tool trajectory in circular milling

in clockwise direction. The chip load at h_{max} generates maximum cutting force and is considered for the calculation of cutting coefficients as indicated in Eq. 7 and 8. h^* is the side edge of the uncut chip thickness generated because of the helical flute profile and also circular motion of the tool trajectory.

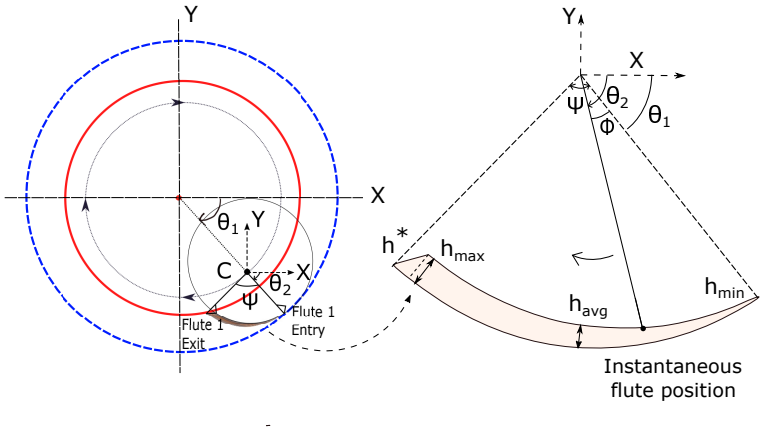

Fig. 2: Chip geometry in circular milling

The local position of the flute in circular milling can be expressed relating to tool trajectory position as indicated below:

$$\phi(\theta_1, \theta_2, i) = \theta_2 - \theta_1 - (i-1)\phi_p \tag{9}$$

Equation 6 can be rewritten considering instantaneous position of the flute at angle ϕ calculated, in this case, as also a function of θ_1:

$$h(\phi) = f_z \sin\left(\phi(\theta_1, \theta_2, i)\right) \qquad \text{if} \qquad \phi \leq \psi \tag{10}$$

The forces measured during experiments by the dynamometer are in XY referential frame: F_X and F_Y as shown in Figure 1(a). The tool rotates around the hole center O in clockwise direction given by angular position θ_1 and around its own axis given by θ_2, also in clockwise direction. The forces F_X and F_Y can be transformed using a rotation matrix (Eq. 11) to deduce F_{tan} and F_{rad} at the tool center. F_{tan} and F_{rad} are significant to understand tool deflection effects on hole quality. To calculate F_t and F_r at the cutting edge, the rotation matrix as a function of θ_2 and the dynamometer referential frame components (F_X and F_Y) presented in Eq. 12 can be applied. The specific cutting coefficients K_c and K_r (N/mm^2) are identified by analyzing F_t and F_r maximum values for a particular set of tool revolutions using Eq.7 and Eq.8.

$$\begin{bmatrix} F_{rad} \\ F_{tan} \end{bmatrix} = \begin{bmatrix} Cos(-\theta_1) & -Sin(-\theta_1) \\ Sin(-\theta_1) & -Cos(-\theta_1) \end{bmatrix} \cdot \begin{bmatrix} F_X \\ F_Y \end{bmatrix} \tag{11}$$

$$\begin{bmatrix} F_t(\theta_2) \\ F_r(\theta_2) \end{bmatrix} = \begin{bmatrix} -Sin(-\theta_2) & -Cos(-\theta_2) \\ -Cos(-\theta_2) & -Sin(-\theta_2) \end{bmatrix} \cdot \begin{bmatrix} F_X \\ F_Y \end{bmatrix} \tag{12}$$

Materials and Methods

In this section, circular milling experiments in Aluminium (2017A) alloy and Titanium (Ti6Al4V) alloy workpieces measuring cutting forces are presented along with external sensor integration. The experiments were carried out for a specific range of cutting conditions, following the experimental setup and the design of experiments described below.

Experimental setup

Circular milling experiments were carried out on a CNC milling center DMU85-DMG mono block machine. The tool used for the experiment is carbide end mill of 8 mm diameter from Fraisa [20]. A prehole of 11 mm diameter is already drilled before by a drill tool. The workpieces were fixed on a 9257B Kistler dynamometer, as shown in figure 3(a), using only its internal measuring region, connected to a 5070 Kistler amplifier. Figure 3(b) shows Titanium alloy sample with milled dimensions. Analogical data of force is converted to digital using a 9201 National Instruments acquisition module with 10 kHz acquisition rate. The measured forces were filtered using a low pass Butterworth filter with cutoff frequency of 700 Hz (appropriated to the maximum spindle speed). In order to detect cutting flute position, an external photoelectric sensor (reference: WL150-P132 from Sick) is connected to a DC power supply and the sensor output is connected to data acquisition card NI 9215 from National Instruments via BNC cable. Sensor data is read and written on Labview platform connected to NI DAQ through USB. The CNC milling center in use has Sinumerik controller from Siemens which is connected to Sinucom NC Trace software via ethernet connection to trace machine related data. The working principle of external sensor along with tracing of machine data is explained in the next subsection.

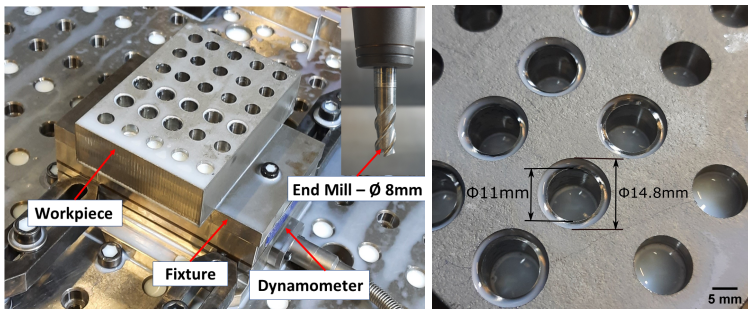

(a) Experimental elements (Tool, workpiece, Fixture and Dynamometer)

(b) Milled dimensions: 14.8 and 11.0 mm (in Titanium)

Fig. 3: Experimental setup

Cutting edge position identification

The external photoelectric sensor is utilized to detect flute position by the principle of light emission and detection on a reflective tape attached to the tool holder as shown in figure 4(b). The sensor produces a voltage high when it detects reflective tape positioned in line with the cutting flute. Also, the CNC machine has a spindle encoder reference (defined by the machine builder) which is used to identify the spindle position in rotary motion. This is illustrated in figure 4(a). It should be noted that

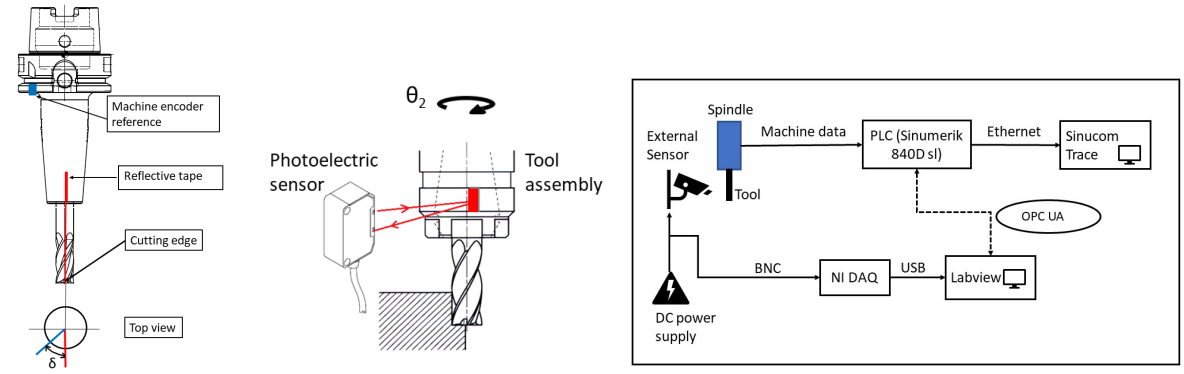

(a) δ identification (b) External sensor operation (c) Instrumentation Schematic

Fig. 4: Cutting flute angular position identification

there is no physical identification mark of encoder reference on the actual machine spindle but it is internally defined by the machine builder. The spindle position data can be traced in real time from the CNC machine by Sinucom Trace. The position of the reflective tape is cross checked and validated by making a test cut in order to compare flute position and force peak at a particular time stamp.

The data from the external sensor and machine trace is analysed to find the angular relation (δ) between the cutting flute position and machine encoder reference point in order to deduce cutter rotation angle θ_2 as shown in the figure 4(a). Figure 4(c) shows the schematic of instrumentation setup in order to acquire the real time data from the CNC machine as well as external photoelectric sensor. In order to precisely deduce the angular relation between cutting flute position and machine encoder point, it is significant to read both of acquired data (Machine data and external sensor data) on the same platform in the same time frame. PLC from the CNC machine can be integrated to Labview via OPC UA [1] [21] which can facilitate to access machine data on Labview along with external sensor data. Our work is ongoing in order to integrate data acquired from different platforms in a common window like OPC UA for better decision making.

This article used a method to deduce δ (Fig. 4(a)) by identifying the common time stamps from two systems and then comparing the signals obtained in the same time frame. Clock from external sensor system and machine trace system is set identical. The set of data points having common time stamps from both the systems is then super imposed as shown in the Figure 5 to identify angular difference between cutting flute and spindle encoder reference position. The sensor signal peak in the graph denotes a cutting flute detection and the corresponding value of the spindle position is found to be consistently between $153 - 158^o$. Since, the above technique involves integrating two separate platforms with different time frames, the value of δ identified varies in a range but this work proposes novel ways to identify cutting edge position in real time for application in smart machining techniques.

Design of experiments

Table 1 summarizes the cutting conditions on Aluminium and Titanium along with tool details for circular milling operations. The machining responses were compared for a constant cutting velocity and a range of feed rates as indicated in the Table 1. Feed as low as 0.02 mm/tooth which is the minimum feed value for any monoblock carbide tool to perform is included in the cutting parameters range. Each test is repeated twice and care is taken that, same feed rate test is not carried out successively twice but in a random order, to eliminate chances of rapid tool wear (if any) at higher feed rate values. Circular milling was carried out on the previously drilled hole with an axial depth of 1 mm and a radial width of cut of 1.9 mm. This leads to a final milled hole diameter of 14.8 mm in order to have a cutting continuity coefficient c less than 1 [22].

[1] Open Platform Communication Unified Architecture

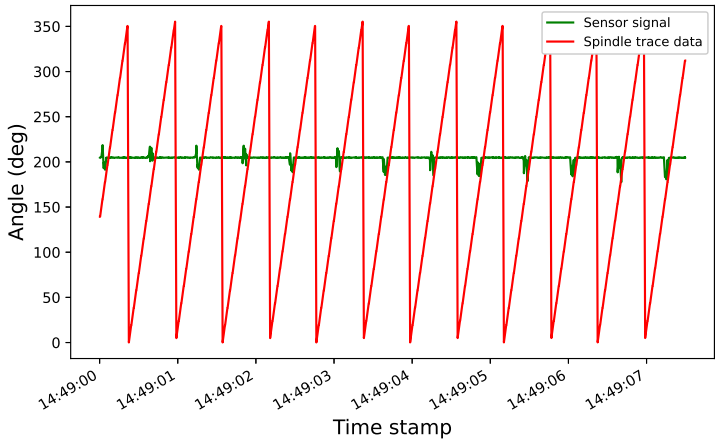

Fig. 5: Identification of δ

Table 1: Design of Experiments: Cutting conditions

Operation	Workpiece	Cutting speed (m/min)	Feed per tooth (mm/th)
Milling ($\varnothing$8 mm, 4 flutes, $\lambda = 30^o$)	Aluminium	40	0.02 / 0.10 / 0.18
	Titanium	40	0.02 / 0.10 / 0.18

Experimental Results

The following subsections present the results of experimental forces for circular milling. Circular milling forces are presented in terms of tool angular position θ_1 (around O) which is taken as a reference for all the feed rates and cutting speed values tested. It should be noted that the trajectory rate ($\theta_1/time$) changes based on variation in feed rate values.

Forces in circular milling

The forces components F_X and F_Y obtained with the dynamometer during circular milling can be seen in the Figure 6. The graph shows the variation of force components (XY reference on the dynamometer) along time, represented by the tool trajectory angle θ_1.

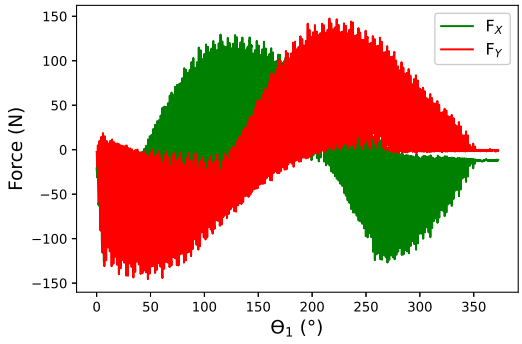

Fig. 6: Experimental forces F_X and F_Y during circular milling of Aluminium as an example (f_z-0.1 mm/th and V_c-40m/min)

Figure 7 shows tangential (F_t) and radial (F_r) forces components (aligned to the cutting edge) and its variation along θ_1 evolution. A window of two tool revolutions is presented (one revolution : $\theta_2 = [0 - 360^o]$). Eight peaks can be observed in the cutting force components for a 4 flute end mill for

Aluminium and Titanium alloys experiments. The cutting forces from dynamometer were transformed as previously indicated in Eq. 12. Each peak corresponds to cutting flute (Fl_i) and swept angle (ψ_i) as shown in the figure 7(a).

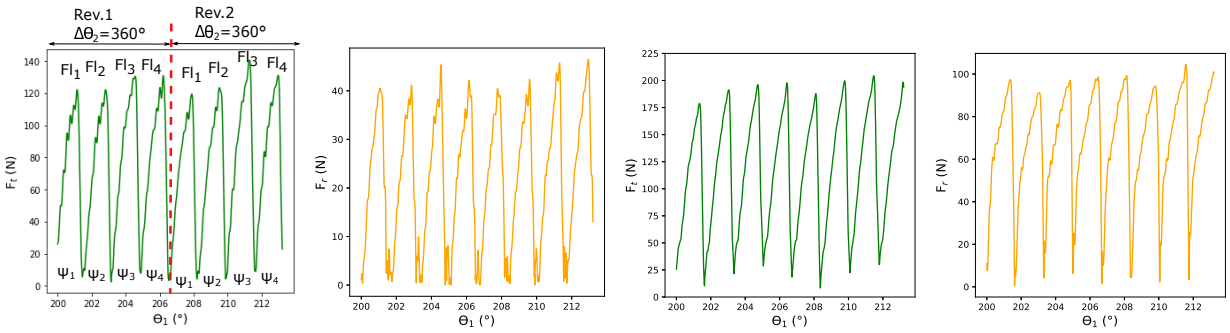

(a) F_t for Aluminium. (b) F_r for Aluminium. (c) F_t for Titanium. (d) F_r for Titanium.

Fig. 7: Calculated F_t and F_r during 2 revolutions in circular milling of Aluminium and Titanium (window on $\theta_1 = [200^o - 213^o]$) at $f_z = 0.1$ mm/th and $V_c = 40$ m/min

Identification map

After acquiring the experimental forces for circular milling, the specific cutting force coefficients were estimated. They are presented in the form of identification map in this section. It is important to claim that the circular milling experiments were done on pre drilled hole. As one of the the goal of this paper is the material identification based on the data, the range of feed per tooth was narrowed to 0.10 and 0.18 mm/th, where the values of forces were closer. Also, low feed rate values as 0.02 mm/tooth are very rarely used in the industry for these materials.

K_c and K_r values are estimated by considering maximum values of F_t and F_r values respectively, for a specific set of tool revolutions. Figure 8 shows the identification map of specific cutting coefficients estimated for Aluminium and Titanium alloys. The data includes values calculated at several tool angle positions θ_1 at different feed rates and constant cutting velocity with the objective of having a representative value with larger spectrum of experimental variability and noise. A clear distinction between both materials and force coefficient values can be identified in different regions of the map presented in Fig.8. Thus, the clear distinction between Titanium and Aluminium regions presented in identification map, can be further applied for material identification in smart machining processes.

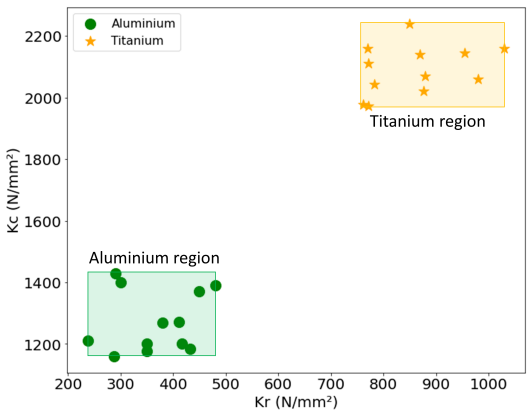

(a) K_c and K_r (Milling)

Fig. 8: Identification Map for Circular Milling in Aluminium and Titanium

Conclusions

The article focuses on kinematics of circular milling and introduces a model to identify cutting coefficients for developing an identification map in smart machining applications. This work also proposes an idea of detecting cutting flute position in real time for instantaneous calculation of cutting forces and specific coefficients. Research is ongoing in order to improve the accuracy of this model since it involves integrating two different data acquisition platforms with its own time frame. However, proposed method could still identify approximately angular difference between cutting flute and spindle reference position which can be interesting for online monitoring applications.

The specific force coefficients are identified in different regions of the map for Titanium and Aluminium due to the materials distinct machinability. Hence, the gap between the cutting force coefficients for both materials makes it suitable for applying smart machining techniques using data monitoring in hole making processes of stacked materials made out of Aluminium and Titanium.

Similar data maps can be developed in orbital drilling by online monitoring of cutting force and cutting flute position for material identification in stacked aerospace applications of Aluminium and Titanium alloys.

References

[1] Zhaoju Zhu, Kai Guo, Jie Sun, Jianfeng Li, Yang Liu, Yihao Zheng, and Lei Chen. Evaluation of novel tool geometries in dry drilling aluminium 2024-T351/titanium Ti6Al4V stack. *Journal of Materials Processing Technology*, 259:270–281, September 2018.

[2] L K Gillespie. Burrs produced by drilling. Technical report, The Bendix Coporation, 8 1976.

[3] Robson Bruno Dutra Pereira, Lincoln Cardoso Brandão, Anderson Paulo de Paiva, João Roberto Ferreira, and J. Paulo Davim. A review of helical milling process. *International Journal of Machine Tools and Manufacture*, 120:27–48, September 2017.

[4] Francisco Puerta Morales, Jorge Gómez, and Severo Raul Fernandez Vidal. Study of the Influence of Helical Milling Parameters on the Quality of Holes in the UNS R56400 Alloy. *Applied Sciences*, 10:845, January 2020.

[5] D. Sun, Patrick Lemoine, Daniel Keys, Patrick Doyle, Savko Malinov, Qing Zhao, Xuda Qin, and Yan Jin. Hole-making processes and their impacts on the microstructure and fatigue response of aircraft alloys. *The International Journal of Advanced Manufacturing Technology*, 94, 2018.

[6] Alexandra Lacombe. *Influence du procédé de perçage sur l'intégrité de surface et la tenue en fatigue de pièces percées en AA2024-T351*. Theses, Université Paul Sabatier - Toulouse III, January 2021.

[7] H. Cao, H. Zhang, and X. Chen. The concept and progress of intelligent spindles: A review. *International Journal of Machine Tools and Manufacture*, pages 21–52, 2017.

[8] N. Geier, P. Davim, and T. Szalay. Advanced cutting tools and technologies for drilling carbon fibre reinforced polymer (cfrp) composites: A review. *Applied Science and Manufacturing*, 2019.

[9] Andrea Pardo, Robert Heinemann, Nuno Miguel Nobre, and Luke Bagshaw. Assessment of decision-making algorithms for adaptive drilling of aerospace stacks. *Procedia CIRP*, 99, January 2021.

[10] Qiang Fang, Ze-Min Pan, Bing Han, Shao-Hua Fei, Guan-Hua Xu, and Ying-Lin Ke. A Force Sensorless Method for CFRP/Ti Stack Interface Detection during Robotic Orbital Drilling Operations. 2015.

[11] Eric Wenkler, Frank Arnold, Albrecht Hänel, Andreas Nestler, and Alexander Brosius. Intelligent characteristic value determination for cutting processes based on machine learning. *Procedia CIRP*, 79:9–14, January 2019.

[12] E. J. A. Armarego and N. P. Deshpande. Computerized Predictive Cutting Models for Forces in End-Milling Including Eccentricity Effects. *CIRP Annals*, 38(1):45–49, January 1989.

[13] D. Montgomery and Yusuf Altintas. Mechanism of Cutting Force and Surface Generation in Dynamic Milling. *Journal of Engineering for Industry*, 113, May 1991.

[14] Avisekh Banerjee, Hsi-Yung Feng, and Evgueni V. Bordatchev. Geometry of chip formation in circular end milling. 59:21–35, March 2012.

[15] Baohai Wu, Xue Yan, Ming Luo, and Ge Gao. Cutting force prediction for circular end milling process. *Chinese Journal of Aeronautics*, 26(4):1057–1063, August 2013.

[16] Maria Clara Coimbra Gonçalves, Gilmar Ferreira Batalha, Yann Landon, and Anna Carla Araujo. Smart drilling: material identification using specific force map. In *11º COBEF*, pages 1–7, Curitiba, Brazil, May 2021.

[17] Y Altintas. Manufacturing Automation: Metal Cutting Mechanics, Machine Tool Vibrations, and CNC Design. *Applied Mechanics Reviews*, 54(5):B84–B84, 09 2001.

[18] Martellotti M.E. An analysis of the milling process. *Trans. ASME*, pages 677–687, 1941.

[19] Anna Carla Araujo, Guillaume Fromentin, and Gerard Poulachon. Analytical and experimental investigations on thread milling forces in titanium alloy. *International Journal of Machine Tools and Manufacture*, 67:28–34, 2013.

[20] Fraisa. Catalogue fraisa. `https://www.fraisa.com/fr/produits/outils-de-fraisage`, 2020.

[21] Chao Liu, Hrishikesh Vengayil, Yuqian Lu, and Xun Xu. A Cyber-Physical Machine Tools Platform using OPC UA and MTConnect. *Journal of Manufacturing Systems*, 51, April 2019.

[22] Anna Carla Araujo and Guillaume Fromentin. Modeling thread milling forces in mini-hole in dental metallic materials. *Procedia CIRP*, 58:623–628, 2017.